Antiarrhythmic versus Arrhythmogenic Potentials of Mesenchymal Stem Cells, Paracrine Factors, and Cardiogenic Cells

Hye Jin Hwang

Department of Medicine

The Graduate School, Yonsei University

Antiarrhythmic versus Arrhythmogenic Potentials of Mesenchymal Stem Cells, Paracrine Factors, and Cardiogenic Cells

Hye Jin Hwang

Department of Medicine

The Graduate School, Yonsei University

Antiarrhythmic versus Arrhythmogenic Potentials of Mesenchymal Stem Cells, Paracrine Factors, and Cardiogenic Cells

Directed by Professor Moon-Hyoung Lee

The Doctoral Dissertation
submitted to the Department of Medicine,
the Graduate School of Yonsei University
in partial fulfillment of the requirements for the degree of
Doctor of Philosophy

Hye Jin Hwang
December 2013

This certifies that the Doctoral Dissertation of
Hye Jin Hwang is approved.

Thesis Supervisor : Moon-Hyoung Lee

Thesis Committee Member#1 : Boyoung Joung

Thesis Committee Member#2 : Daehyeok Kim

Thesis Committee Member#3: Jong Eun Lee

Thesis Committee Member#4: Sahng Wook Park

The Graduate School
Yonsei University

December 2013

ACKNOWLEDGEMENTS

I thank my supervisor, Dr. Moon-Hyoung Lee for helping my knowledge extend broadly from clinical science to basic science, and thank researchers in Yonsei cardiovascular research center for helping this project thoroughly.

I sincerely thank my old professor, Dr. Sung Soon Kim, who introduced to me the exciting academic field of electrophysiology to make me devote my life.

I thank my husband, Dr. Jae Keun Kim, with whom I have talked and shared many fascinating ideas so far.

Lastly, I thank God with my whole heart to teach me and guide my way.

<TABLE OF CONTENTS>

LIST OF FIGURES

ABSTRACT

Thesis title: Antiarrhythmic versus Arrhythmogenic Potentials of Mesenchymal Stem Cells, Paracrine Factors, and Cardiogenic Cells

Hye Jin Hwang

Department of Medicine
The Graduate School, Yonsei University

(Directed by Professor Moon-Hyoung Lee)

The purpose of this study was to evaluate the anti-arrhythmic potential of mesenchymal stem cells (MSCs), paracrine media (PM) secreted from MSCs and cardiogenic cells differentiated from MSCs. To investigate the effect of MSCs, paracrine factors secreted from MSCs, and cardiogenic cells differentiated from MSCs on arrhythmogenicity in rats with MI, we injected PM secreted under hypoxic-, normoxic conditions (hypoxic PM and normoxic PM), MSCs, and cardiogenic cells into the border zone of infarcted myocardium in rats. We found that the injection of hypoxic PM, but not normoxic PM, markedly restored conduction velocities, suppressed focal activity, and prevented sudden arrhythmic deaths in rats. Underlying this electrophysiological alteration was a decrease in fibrosis, restoration of connexin 43, alleviation of Ca^{2+} overload, and recovery of Ca^{2+}-regulatory ion channels and proteins, all of which is supported by proteomic data showing that several paracrine factors including bFGF, IGF-1, HGF, and EF-hand-domain-containing 2 are potential mediators. MSCs injection did not reduce or prevent arrhythmogenicity, suggesting that anti-arrhythmic or pro-arrhythmic potential of MSCs is mainly dependent on paracrine factors. In contrast, cardiogenic cells injection reduced arrhythmogenicity by improving conduction velocity and acquiring homogeneity of conduction vector. Paracrine molecules of MSCs depending on surrounding environment, hypoxic or normoxic status, determines anti-arrhythmic potential of MSCs. MSCs did not affect arrhythmogenicity but cardiogenic cells differentiated from MSCs had anti-arrhythmic effect by attenuating tissue inhomogeneity.

Key words: ventricular tachyarrhythmia; mesenchymal stem cells; myocardial infarction; paracrine factors; cardiogenic cell

Antiarrhythmic versus Arrhythmogenic Potentials of Mesenchymal Stem Cells, Paracrine Factors, and Cardiogenic Cells

Hye Jin Hwang

Department of Medicine
The Graduate School, Yonsei University

(Directed by Professor Moon Hyoung Lee)

I. INTRODUCTION

Advances in stem cell biology provide a basis for potential cell therapy to cure myocardial infarction. In spite of early success reports, there are inconsistencies regarding the therapeutic benefits of mesenchymal stem cells (MSCs)-based therapy for myocardial infarction (MI) (1). Cellular heterogeneities caused by stem cell injection may increase arrhythmogenesis (2,3), while growth factors and cytokines released from transplanted MSCs may be beneficial (4,5). Although stem cell therapy has emerged as a promising option to repair impaired contractile function, confounding issues concerning the pro-arrhythmic and anti-arrhythmic potentials of stem cell therapy have led to intense discussion.

The pro-arrhythmic potentials by MSCs can be attributed to tissue heterogeneity by transplantation of unexcitable MSCs (2), possible heterogeneous sympathetic nerve sprouting (6), teratoma formation, and spontaneous focal activity. The inconsistent results may be due to varying circumstances surrounding implantation sites. However, little is known about how environmental status affects the potential role of stem cells, particularly with respect to their ability to prevent arrhythmogenicity.

This investigation focused on whether paracrine factors released from MSCs could modulate the electrophysiological properties of the border or ischemic zone, creating spontaneous focal activity through impaired intracellular Ca (Ca_i) handling (7,8) or reentrant arrhythmia (9). The present study also sought to evaluate the direct effect of MSCs by comparing MSCs-engrafted rats with rats treated with cardiogenic cell differentiated from MSCs.

II. MATERIALS AND METHODS

Preparation of paracrine media Paracrine media (PM) was prepared as follows: 90% confluent second passage MSCs were fed with serum-free Dulbecco's Modified Eagle Medium (DMEM). MSCs (1×10^6 cells) were cultured for 12 hours under hypoxia or normoxia. The media of MSCs cultured under hypoxia was defined as hypoxic PM, and media cultured under normoxia as normoxic PM, and both were assumed to contain various paracrine molecules. Hypoxic PM and normoxic PM were collected. Hypoxic conditions were created by incubating cells at 37℃ in an anaerobic system (Technomart INC., Korea) with a 5% CO_2, 5% H_2, and 85% N_2 atmosphere, and a chamber oxygen level of 0.5%. A colorimetric redox indicator (CRI) solution (resazurin, 89%, Sigma) was used to ensure that hypoxic conditions were maintained. For injection, conditioned medium from 1×10^6 cells was centrifuged to remove cell debris and concentrated by VIVASPIN6 (Vivascience Ltd., Scottsdale, AZ). The medium was continuously centrifuged a 1000 x *g* for 30 minutes at 4℃ using an ultracentrifuge.

***Ex vivo* modification of MSCs.** To differentiate MSCs into cardiogenic cells, MSCs at passage 2 were seeded in 60 mm plate at 2×10^5 cells/ml and treated with 1 μM PMA (Sigma) at a final concentration. The media was replaced with fresh PMA-containing media every three days for up to nine days.

Myocardial infarction induction and treatment of hypoxic PM, normoxic PM, MSCs, and cardiogenic cells All animal experimental procedures were approved by the Committee for Care and Use of Laboratory Animals, Yonsei University College of Medicine, and performed in accordance with the Guidelines and Regulations for Animal Care. Myocardial infarction was produced in male Sprague-Dawley rats (250-300 g) by left anterior descending (LAD) coronary artery ligation, as described above. Briefly, after anesthesia with ketamine (10 mg/kg) and xylazine (5 mg/kg), hearts were exteriorized by opening the chest at the third and fourth ribs. After 1 hour of occlusion, the infarcted heart was reperfused and sham (saline), hypoxic PM, normoxic PM, MSCs, or cardiogenic cells were injected at the border region. Hypoxic PM or normoxic PM of MSCs (1×10^6 cells) was enriched to 100 μl and injected into the infarct border region in three different sites using a syringe with a 30-gauge needle. For MSC or cardiogenic cells transplantation, cells (1×10^6 cells) were suspended in 10μl of serum-free medium and injected into the border in the same way. Rats that expired during the procedure or immediately after cell implantation were excluded for sudden death mortality. For identification of arrhythmic death as the cause of death, rats were monitered by a telemetry and autopsies were performed with these rats to confirm that the animals did not expire

from cardiac rupture. Experimental groups were used for surface electrocardiography (ECG), telemetric monitoring, *in vivo* isoproterenol test, optical mapping, Millar catheterization, and morphologic analysis at 11 days after injection of hypoxic PM, normoxic PM, MSCs, or cardiogenic cells.

Optical mapping For optical mapping, hearts were excised, retrogradely perfused through the aorta with Tyrode's solution gassed with 95% O_2 and 5% CO_2, and stained with a voltage sensitive dye, di-4-ANEPPS (Invitrogen Corporation, Carlsbad, CA). Hearts were placed in a chamber to maintain 37.0 ± 0.2℃, and 5 μM blebbistatin was added to the perfusate to reduce movement artifacts. Excitation light was delivered by epi-illumination with two green LED lamps (500 ± 30 nm, LL-50R30-G25, Optronix, Seoul, Korea). Fluorescence images from the anterior surface of the heart were recorded with a CCD camera (128 x 128 pixels, Dalsa Inc., Billerica, MA) and the field of view was 1.0 x 1.0 cm^2 with a spatial resolution of 78 x 78 μm^2. The sampling rate was 420 frames /sec. The rhythm of optical recordings was continuously monitored by ECGs obtained with widely spaced bipoles, one at the apex of the left ventricle and the other at the high lateral wall of the right ventricle, using a Biopac System (BIOPAC Systems Inc.). Fluorescence recordings were filtered with a Gaussian filter (3 x 3 pixels) in the spatial domain, and first order derivatives (dF/dt) were calculated using a polynomial filter (3^{rd} order, 13 points) in the temporal domain. Activation time-points at each site were determined from $(dF/dt)_{max}$, and isochronal maps of activation were generated. The duration of the action potential at 80% repolarization (APD_{80}) was measured. Conduction velocity (CV) within the border or normal regions was measured under point stimulation at a cycle length of 280 ms for 20 beats. Local CV vectors were estimated from each pixel's seven nearest neighbors in the activation time of its temporal wave. To improve the signal-to-noise ratio, the local CV was spatially filtered using a 7 x 7 nearest-neighbor Gaussian convolution kernel and the acute change in its magnitude was suppressed using log-transformation (10,11). A CV map of the anterior surface of the heart focused by CCD camera was derived from local CV. Border zones were identified from activation map where slow conduction occurred. Infarct zones were defined as the area where the voltage signals were near completely absent. Analyses were performed with software using IDL 6.4 (Research Systems, Boulder, CO, USA) and MATLAB (Mathworks, Inc.).

Statistical analysis Data are expressed as means ± SE for continuous variables and as proportions for categorical variables. Statistical analyses of more than two groups were done by one-way ANOVA for parametric variables. Bonferroni adjustment was used for multiple comparisons. Premature ventricular contractions (PVCs) and CV with nonparametric distribution were analyzed by the Kruskal-Wallis test followed by post hoc testing via Mann–Whitney *U* test with Bonferroni adjustment for multiple testing. The chi-square test or the Fisher exact test for categorical variables

was used. Survival was analyzed by the Kaplan-Meier method with the breslow test. A value of $P<0.05$ was considered statistically significant. The SPSS 18.0 statistical package (SPSS Inc., Chicago, Illinois) was used.

Cell culture, *in vivo*, and *in vitro* analyses These methods are provided in detail in the Supplementary Appendix.

III. RESULTS

Paracrine effect of MSCs on Electrical Stability

We studied animals using LV catheterization, ECG, or telemetric monitoring. We found improved LV contractile function and shorter QRS duration in hypoxic PM-treated rats compared to sham-injected rats. In addition, PVCs tended to be suppressed by hypoxic PM treatment (Appendix Fig. 1). We further examined the protective effect of paracrine factors with isoproterenol infusion, which facilitates both early afterdepolarization and delayed afterdepolarization (DAD) (13). For 15 minutes after intraperitoneal injection of isoproterenol (2mg/kg), sustained ventricular tachyarrhythmia (VT) was induced in 1 of 9 sham-injected rats, but not in the hypoxic PM-, normoxic PM-, MSCs-treated rats. Frequent PVCs were induced in the sham-injected animal group, whereas PVCs were significantly reduced in hypoxic PM-treated rats (Fig.1A and 1B).

To further investigate vulnerability to arrhythmias of infarcted hearts injected with paracrine factors, we performed an *ex vivo* electrical vulnerability test using a burst-pacing protocol. No monomorphic or polymorphic VT was observed in non-infarcted control rats (n=10). However, VT were induced 81.8% sham-injected rats (n=11), indicating that localized myocardial infarction markedly enhances induction of VT, allowing a systematic evaluation of how PM secreted from MSCs affects electrical vulnerability. VT occurred in 16.7% of 12 hypoxic PM-treated rats (sham vs. hypoxic PM, $p<0.01$), in 58.3% of 12 normoxic PM-treated rats (normoxic PM vs. hypoxic PM, $p <0.05$), in 46.7% of 15 MSCs-treated rats (MSCs vs. hypoxic or normoxic PM, $p >0.05$) (Fig.1C). VT vulnerability score was also different between hypoxic- and normoxic-PM treatments. In ANCOVA analysis adjusted for LV ejection fraction, the strong association between VT vulnerability and PM treatments was noted (Appendix Fig.2). This supplied evidence of a significant difference of anti-arrhythmic role of PMs secreted from different environments.

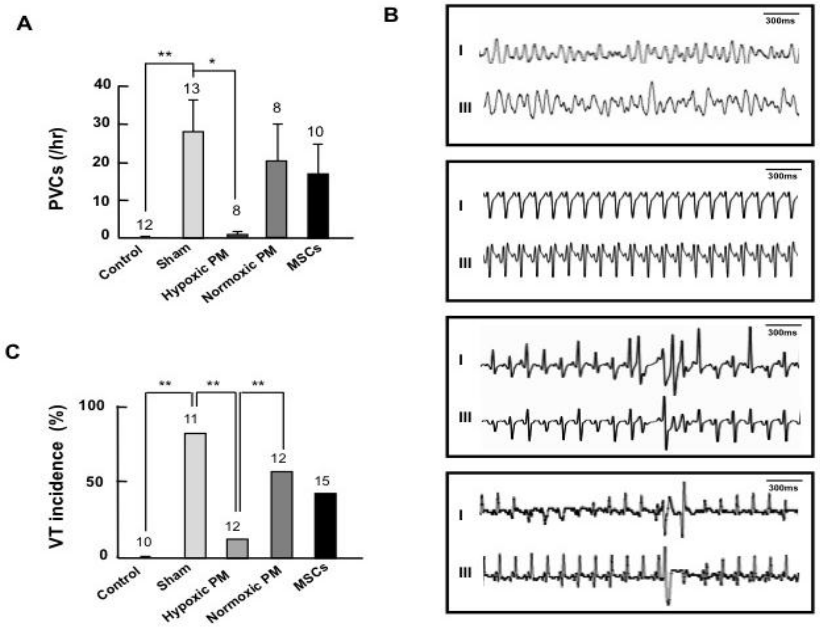

Figure 1. Improvement of survival and VT protection by hypoxic PM

(A) Incidence of sudden death for sham-injected animal (n=23), hypoxic paracrine media (PM)- (n=22), normoxic PM- (n=23) or MSCs-injected rats (n=22) during the 11 days after injury and treatment. Survival was significantly different among 4 groups (**p*<0.05, ***p*<0.01). (B) Numbers of premature ventricular contractions (PVCs) from an *in vivo* isoproterenol test (**p*<0.01, ***p*<0.001, Mann–Whitney *U* test for independent samples). (C) Representative surface ECG recording from an *in vivo* isoproterenol test. Sustained VT was induced in a sham-injected rat (upper). PVCs were rarely observed in hypoxic PM-injected rats (upper middle) and frequent PVCs were noted in normoxic PM- and MSCs-injected rats (lower middle and bottom). (D) VT inducibility. Note strongly reduced susceptibility to VT induction in PM-injected groups compared with sham- or normoxic PM-injected group. Conversely, VT was similarly inducible in normoxic PM- and MSCs-injected rats (** *p*<0.005). Numbers above bars indicate *n*; error bars show s.e

Alteration of electrophysiological properties by paracrine effect of MSCs but not by cellular effect itself

We assessed the electrophysiological impact of paracrine factors on the infarcted myocardium by optical mapping using Langendorff perfusion at 7 to 11 days after injury and treatment. Wave propagation in sham-injected hearts was prominently blocked at the boundaries of the infarcted regions (Appendix Fig. 3, upper panel). In contrast, action potentials initially circumventing the infarct region propagated transmurally in hypoxic PM-treated hearts (Appendix Fig. 3, lower panel). Focal activity arising from the infarct border is a representative electrophysiological feature that triggers arrhythmia in MI (7,8). Spontaneous ectopic beats emanating from the border region at sinus rhythm were observed frequently in 55.6% of sham-injected rats (n=9) (Fig. 2A). However, treatment with hypoxic PM markedly suppressed the ectopic focal beats from the border region (0%, n=6), with normoxic PM treatment (33.3%, n=6) resulting in moderate suppression. In MSCs-treated hearts, the ectopic focal beats were also moderately suppressed (25%, n=8), to similar extent compared to

normoxic PM treated hearts. Local CV was markedly depressed in the border zone of sham-injected hearts and moderately in normoxic PM-treated border, in contrast to the notable restoration of CV seen in hypoxic PM-treated hearts (Fig. 2B). Figure 2C presents the different regional distributions of CV in hypoxic PM- and normoxic PM-treated hearts. CV was also moderately restored in MSCs-treated border zone, to similar extent compared to normoxic PM-treatment (Fig. 2B). In contrast, APD_{80} was significantly different between the MSC-transplanted border zones and normoxic PM-treated border zones. To identify the electrophysiological alteration due to MSC implantation, we confirmed the presence of DAPI-labeled MSCs at the injected sites (Fig. 2D).

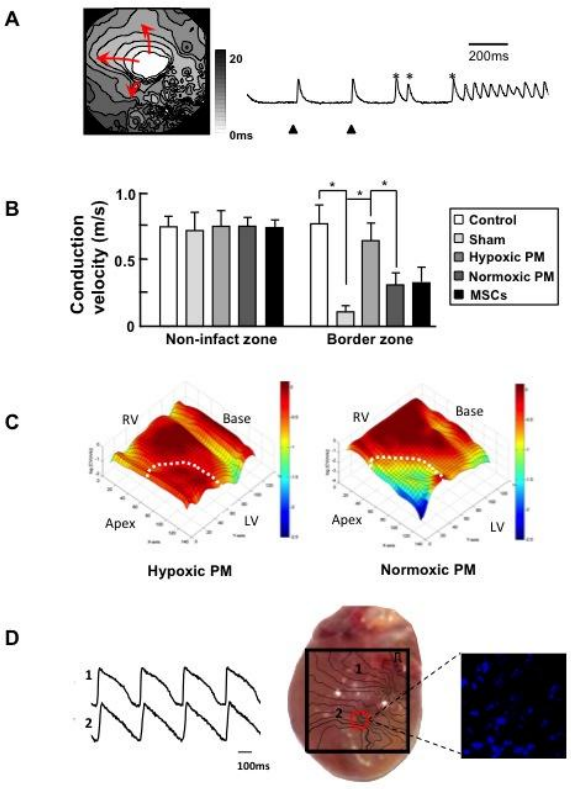

Figure 2. Peri-infarct zone as arrhythmogenic substrate and restoration of conduction by hypoxic PM

(A) The isochronal map (left) shows a focal discharge at the peri-infarct zone. The scale bar indicates local activation times. The action potential recorded from the border zone (right) shows that the focal beats emanating from the border (asterisk) initiate VT. Red arrows indicate the direction of wave front propagation. Black triangles indicate the paced beats. (B) Local conduction velocities (CV). There is a more than five-fold increase within the hypoxic PM–injected border zone compared with sham-injected border zone (*p<0.001, Mann–Whitney U test for independent samples). (C) Representative examples of CV maps in hypoxic PM and normoxic PM-treated region (white circle) (78 m x 78 m). CV within the infarct region was largely elevated in hypoxic PM-injected heart. (D) The action potential recorded in the normal zone and MSC-engrafted zone (site 1 and 2, respectively, in left panel), real heart image with a representative isochronal map during pacing in the MSC-engrafted heart (middle), and DAPI-coated MSCs (right). The black boxes indicate the optical view fields with 10 mm x10 mm. The red circle indicates the MSCs injected site. Immunohistostaining identifies the presence of DAPI-coated MSCs around the injected lesion (right).

Change of electrophysiological substrate by paracrine media

This series of experiments proposes that the enhanced conduction resulting from treatment with hypoxic PM could be attributed to the rescue of hypoxic cardiomyocytes from apoptosis and the subsequent decrease in fibrous tissue (14), which caused slow conduction by a zigzag course of activation, thus facilitating reentry (9). TUNEL-positive myocardial cells were significantly reduced by approximately 50% in hypoxic PM-treated hearts, compared to sham-injected hearts (Fig. 3A). Fibrosis was significantly decreased in hypoxic PM-treated hearts and not noticeably decreased in normoxic PM-treated hearts (Fig. 3B). The degree of fibrosis in MSC-transplanted rats was similar to that in normoxic PM-treated rats (15.1 ± 2% in MSC-transplanted hearts vs. 15.3 ± 1.5% in normoxic PM-treated hearts, $p > 0.05$), implicating that the effects of paracrine action of MSCs in this model might be similar to the effects of normoxic PM. Decreased CV in ischemia is also induced by alterations in gap junction conductance (15). Figure 3C showed that total Cx43 signal in the border zone of post-infarct heart was decreased and was not in the intercalated disk area, and dephosphorylated Cx43 was increased. Hypoxic PM ameliorated dramatically the distribution of total Cx43, whereas the disarray of Cx43 was partially restored by normoxic PM or MSCs injection (Fig.3C). Moreover, dephosphorylated Cx43 fluorescence intensity was moderately decreased with normoxic PM or MSCs treatment but remarkably attenuated by hypoxic PM treatment (Fig.3C). Total amount of Cx 43 decreased in sham-injected area and moderately decreased by normoxic PM-treated border zone, but increased in hypoxic PM-treated border zone (Fig. 3D). decreased with normoxic PM or MSCs treatment but remarkably attenuated by hypoxic PM treatment (Fig.3C).

Alteration of Ca^{2+}-regulatory ion channels and proteins in border zone contribute to trigger easily focal activity and may affect electrical conduction (16,17). We observed a marked decrease in mRNA levels of L-type calcium channel (LTCC), SERCA 2a, Na^{+}/K^{+} ATPase, and the calcium-binding proteins, calreticulin and calmodulin in the border zone, which was significantly restored in hypoxic PM-treated area and moderately in normoxic PM-treated area (Fig 4A). The increased mRNA level of the Na^{+}/Ca^{2+} exchanger (NCX) in border zone, of which increased activity lead to DAD, was completely rescued by hypoxic PM and partially by normoxic PM (Fig. 4A). We did not assess the alteration of Ca^{2+}-regulatory ion channels and proteins in MSCs-transplanted border zone, because ion channels of MSCs are known to be different (18).

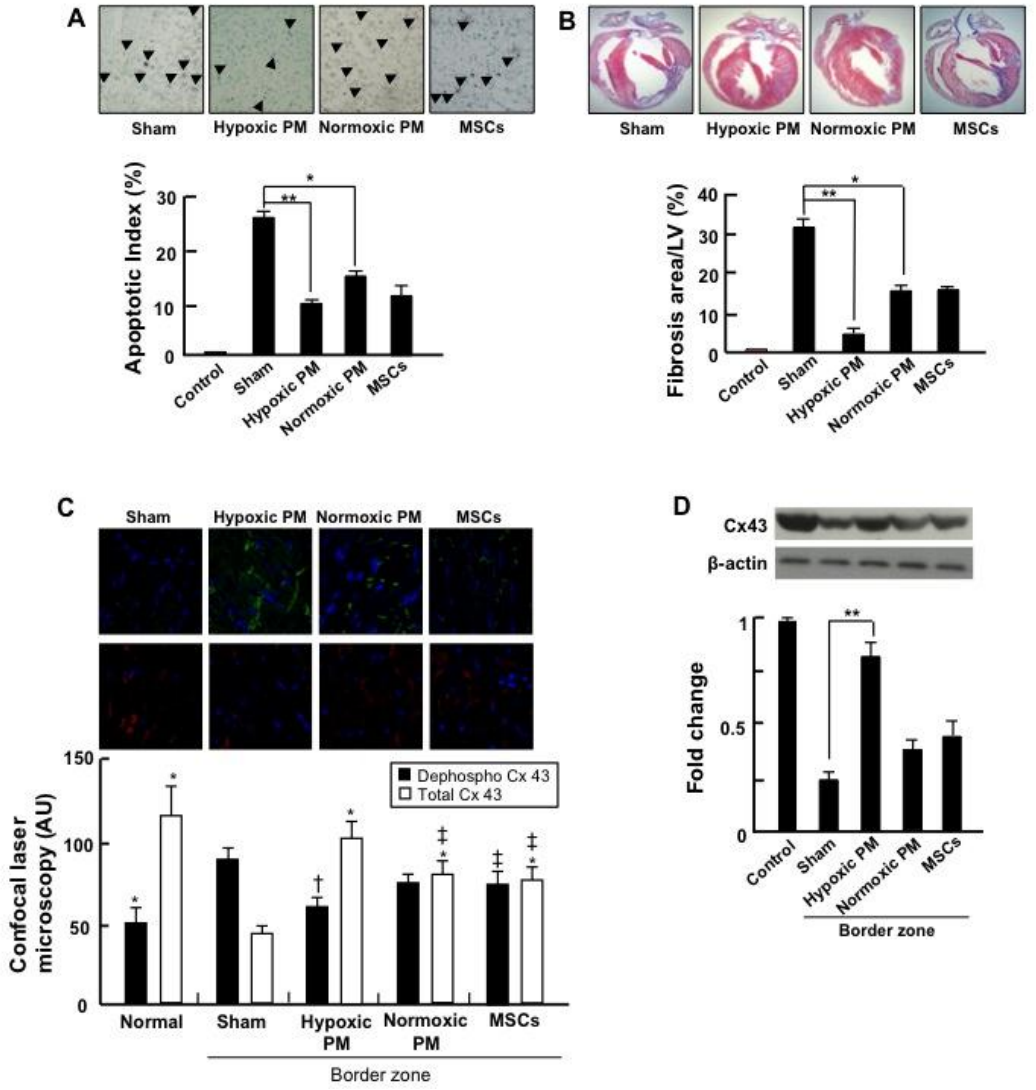

Figure 3. Histological analysis and effects of PM or MSCs on connexin 43 expression. (A) TUNEL assay for apoptotic cells. TUNEL-positive myocardial cells were significantly reduced in hypoxic PM-injected hearts compared to sham-injected hearts (*p<0.01, **p<0.001). (B) Masson's trichrome staining for determination of fibrosis area. Fibrosis was significantly decreased in hypoxic PM-treated hearts and not noticeably decreased in normoxic PM- or MSCs-injected hearts (*p<0.01, **p<0.001).

(C) Immunohistochemistry for Cx 43. In sham-injected hearts, total Cx43 signal (green) decreased and its array was disturbed, whereas dephosphorylated Cx43 signal (red) increased. Hypoxic PM ameliorated dramatically the distribution of total Cx43 and attenuated dephosphorylated Cx43 signal, whereas the disarray of total Cx43 was partially restored by normoxic PM or MSCs injection (*p<0.001 vs. sham, †p<0.01 vs. sham, ‡ p<0.05 vs. hypoxic PM). (D) Western blot analysis for Cx43. The increase of Cx43 expression by hypoxic PM in border zone of infracted heart was noted (**p<0.001)

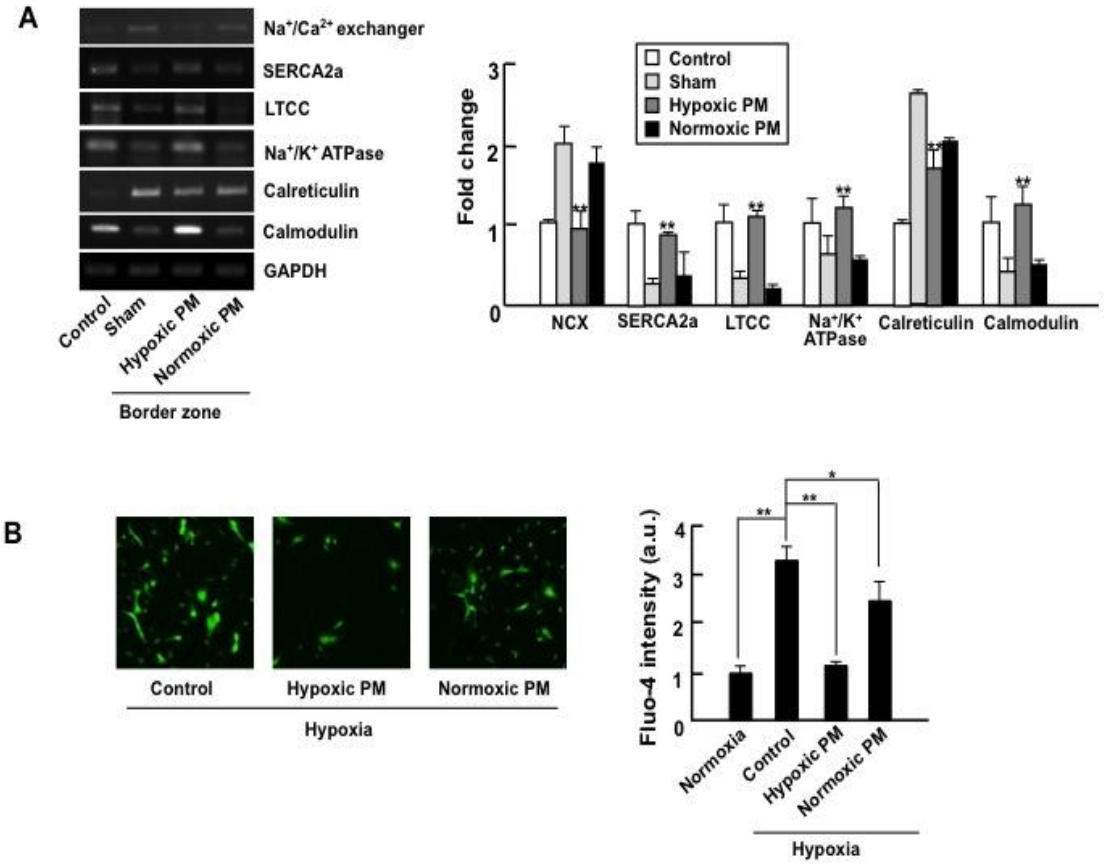

Figure 4. Alteration of Ca^{2+}-regulatory proteins and intracellular Ca^{2+} concentration. (A) Effect of PM on genes coding for ion exchangers and Ca^{2+}-regulating proteins. The mRNA levels of NCX, SERCA2A, LTCC, Na^+/K^+ ATPase, calreticulin, and calmodulin in sham-, hypoxic PM-, normoxic PM-injected border zone were examined by RT-PCR (*p <0.01, **p <0.001). (B) Representative fluorescent images of cytosolic free Ca^{2+} and relative fluorescence intensity in sham-, hypoxic PM- and normoxic PM-treated hypoxic cardiomyocytes (*p <0.01, **p <0.001).

Different action of hypoxic PM and normoxic PM *in vitro* study

For *in vitro* study, cardiomyocytes (2 x 10^6) was subjected to 3 hr of hypoxia followed by reperfusion and treatment of hypoxic or normoxic PM. We also evaluated survival and change of Cx 43 and dephosphorylated Cx 43 in ischemic cardiomyocytes with no treatment, treated by hypoxic or normoxic PM, which was consistent with *in vivo* study results (Appendix Fig.4).

Next, alterations in Ca_i were examined, because focal activity is easily induced by Ca^{2+} overload in an ischemic setting. A significant increase in fluorescence intensity was seen in hypoxic cardiomyocytes, indicating Ca^{2+} overload. However, hypoxic PM decreased the fluorescence intensity by 65% compared to controls, and produced a two-fold decrease compared to normoxic PM (Fig. 4B).

In addition, we observed mRNA expression levels of LTCC, SERCA 2a, Na^+/K^+ ATPase, calreticulin, calmodulin, and NCX, which were consistent to *in vivo* study (Appendix Fig.5).

Different expression of paracrine factors secreted under hypoxic and normoxic environment

We then performed proteomic analysis to identify the paracrine factors that were responsible for the differences between hypoxic PM and normoxic PM. As shown in online Table 5, the secreted levels of the growth factors bFGF, IGF-1, and HGF differed between hypoxic PM and normoxic PM. bFGF, which stimulates Cx43 (19), regulates intracellular Ca^{2+}, and is related to anti-apoptosis (20), which was 8-fold higher in hypoxic PM than in normoxic PM (Appendix Fig. 6). The level of IGF-1, which has been shown to be related to Cx43 expression (21), and HGF, anti-fibrotic and anti-apoptotic factor (22,23) were elevated in hypoxic PM compared to normoxic PM (Appendix Fig.6). Moreover, EF-hand-domain-containing 2, reticulocalbin 2, secreted modular calcium-binding protein 1 (Smoc 1), and secretogranin II, which are known to regulate calcium homeostasis (24-27), were detected only in hypoxic PM (Table S1).

Cardiogenic cells differentiated from MSCs by a protein kinase C activator.

In a previous study, we showed that small chemical molecules, including protein kinase inhibitors, recognizably change stem cell fate (13). After screening 189 such small chemicals, we found that PMA, a PKC activator, specifically induced the expression of cardiogenic markers as revealed by sandwich ELISA (Fig. 5A). Immunocytochemical staining showed increased fluorescence of cardiac-specific markers such as cardiac troponin T (cTnT), myosin light chain (MLC), and myosin heavy chain (MHC), but levels of the MSC specific marker CD90 were lower after nine days in the cardiogenic cells produced by PMA (Fig. 5B). In addition, we observed that the expression of cardiac specific transcription factor, NkX2.5, was also significantly upregulated in the cardiogenic cells using sandwich ELISA (Fig. S7). Interestingly, the fluorescence of connexin 43 (Cx43), a gap-junction, was markedly increased in the cardiogenic cells (Fig. 5B). We observed that the cardiac phenotypes were similarly upregulated in the cardiogenic cells (Fig. 5C), indicating that PMA endows MSCs with more homogeneous cardiogenic properties. The expressions of SERCA and LTCC, were also significantly increased in the cardiogenic cells, but not in control MSCs, in a time dependent manner (Fig. 5D). This observation suggests that the activation by PMA triggers a cascade of transcriptional activation that regulates the differentiation of MSCs into cardiomyocytes.

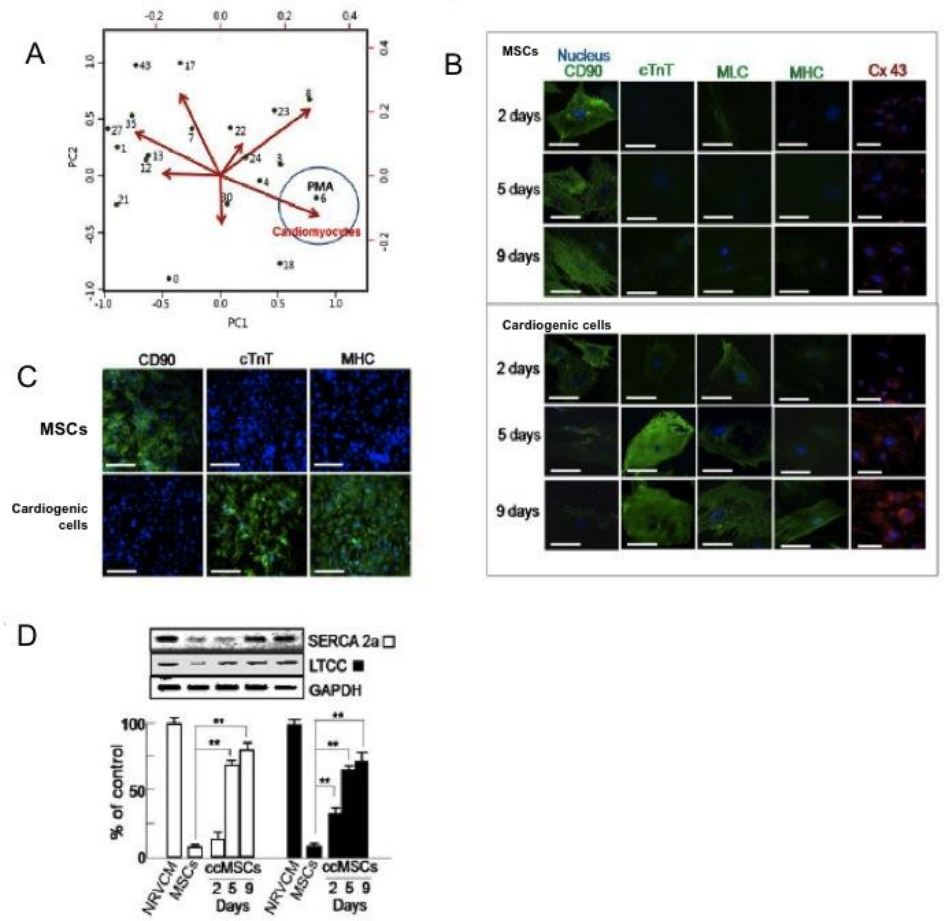

Figure 5. Characterization of cardiogenic cells derived from PKC-activated MSCs (A) Principal component analysis (PCA) for small molecule-induced modification of MSCs. (B) Immunocytochemical determination for the altered expression of the MSC-specific marker CD90 and cardiac-specific markers cTnT, MLC, MHC, and Cx43, in control MSCs and the cardiogenic cells at the designated days after treatment (scale bar=50 μm, magnification: 400x). (C) Immunocytochemical analysis for the homogenic characterization of the cardiogenic cells. Blue indicates nuclei and green is FITC for specific cardiac markers (scale bar=250 μm, magnification: 100x). (D) The altered expression of Ca^{2+} homeostasis-related proteins SERCA 2a and LTCC in MSCs and the ccMSCs. All data are expressed as means±SEM. *p<0.05, **p<0.01.

Electrophysiological properties by implantation of cardiogenic cells.

In comparison between MSCs and paracrine media, we found that cellular effect of mesenchymal stem cells in terms of arrhythmogeneity is at least minimal, that is neither harmful nor beneficial. We further examined the effect of acquisition of homogeneity by injecting cardiogenic cells differentiated from MSCs. On optical mapping, wave propagation during programmed electrical stimulation from the non-infarct site of the LV base was markedly improved in the cardiogenic cells-engrafted hearts. CV maps revealed marked restoration of CV in the cardiogenic cells-engrafted region with recovery

of local CV (0.71±0.12mm/ms, n=6), in contrast to partial restoration of CV in the MSC-engrafted region (0.38±0.08mm/ms, n=7) (Fig. 6A). The direction of the CV vector was homogeneous in the cardiogenic cells-engrafted site compared to the MSC-engrafted site (Fig. 6B). In an electrical vulnerability test using a burst pacing protocol, VT induction was profoundly suppressed in the ccMSC-engrafted group (13%, n=8 for cardiogenic cells-engrafted group and 46.7%, n=15 for the MSCs engrafted group, respectively). Surface 6-lead electrocardiography (ECG) showed a shorter QRS duration in the cardiogenic cells-engrafted rats compared to MSC-engrafted rats (Fig. 6C), indicating more homogeneous ventricular activation of the cardiogenic cells-engrafted myocardium.

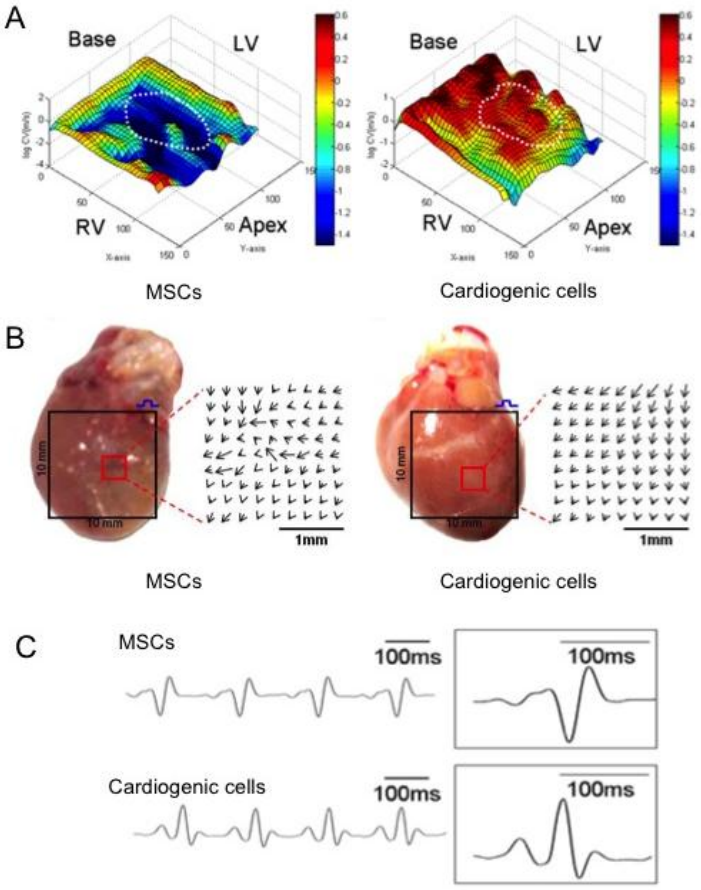

Figure 6. Conduction velocity (CV) and electrogram on the cardiogenic cell-engrafted hearts (A) Representative examples of CV maps in the MSC- and the cardiogenic cells-engrafted hearts(white circle) (78 m x 78 m). (B) Real heart image and CV vector in the MSC- (left) and the cardiogenic cells-engrafted hearts (right). I) Surface ECG recording (lead II) from the MSC- and the cardiogeic cells-engrafted rats.

IV. DISCUSSION

The current study demonstrated that 1) paracrine factors from MSCs depends on the surrounding conditions, specifically whether it is under hypoxic or normoxic condition, 2) paracrine factors released under hypoxic condition have a strong anti-arrhythmic effect by reducing ectopic activity and improving conduction velocity, and 3) cardiogenic cells injection reduced arrhythmogenicity by acquiring tissue homogeneity. To the best of our knowledge, this is the first experimental study to report on the role of paracrine factors on the anti-arrhythmic potential of MSCs and cardiogenic cells.

One of the major challenges facing stem cell therapy is to create tissue heterogeneity, which may potentially increase vulnerability to cardiac arrhythmias. This study provides an alternative therapeutic approach using only paracrine factors or cardiogenic cells.

Fibrotic tissue surrounding surviving cells in infarcted myocardium reduces the speed of impulse propagation, blocks conduction, and facilitates reentry (9). Moreover, fibrosis facilitates the ability to generate triggered activity by a mechanism of sink-source mismatches through coupling between cardiac myocytes and fibroblasts (28). This sequential process was weakened by paracrine growth factors or cytokines from hypoxic MSCs, such as bFGF and HGF, thereby allowing a more synchronized electrical propagation and contraction in hypoxic PM treated hearts. Even though reduced fibrosis and cell death may lead to improvement of contractile function and antiarrhythmic effect, the potency of antiarrhythmic effect of paracrine molecules secreted from MSCs is likely to be more predominant (Fig.S3). Disruption of Cx43 coupling is another main cause of decreased CV in the border zone (15). We determined that the levels of IGF and bFGF secreted from MSCs were significantly increased under hypoxia, and this was associated with increased Cx43 expression (19,21,29), leading to enhanced conduction. Although the current study did not demonstrate the direct association between IGF/bFGF and Cx43 expression, bFGF and IGF were reported to increase expression of connexin 43 and suppress the ventricular arrhythmia in another study (18). We also found that increased intracellular Ca^{2+} concentration was rescued with hypoxic PM. An increase in Ca^{2+} ions in the cell leads to an overload of the sarcoplasmic reticulum (SR), resulting in spontaneous Ca^{2+} ions leakage from the SR. Reduction in intracellular Ca^{2+} by hypoxic PM (Fig. 4B) is in line with reduction of PVCs observed in *in vivo* studies (Fig.1C**).** Moreover, LTCC during decreased gap junction coupling plays an increasing role in propagation (16,17). In our study, a recovery of LTCC by hypoxic PM may contribute to the increased conduction at the border zone.

Despite the antiarrhythmic effects of paracrine factors from MSCs, the inexcitability of MSCs could be regarded as proarrhythmogenic. However, it is difficult to evaluate the direct pro-arrhythmic effect of cells transplanted into the myocardium, independent of the paracrine effect released from injected MSCs. It is assumed that MSCs implanted after 1 hour ligation of the LAD coronary artery would be

more likely under normoxic condition over time. It may be possible to deduce the cellular effect of MSCs in terms of arrhythmogenicity by comparing normoxic PM-treated rats and MSCs-implanted rats**.** Our study demonstrated that the degree of fibrosis, expression level of Cx43 or Ca^{2+} related proteins was not different in MSCs- and normoxic PM-treated hearts, suggesting that MSCs implanted at border zone after ligation and release might release paracrine molecules similar to components of normoxic PM. The current study suggests that the cellular properties of MSCs appear to be neither as beneficial, nor influential, for arrhythmogenicity as paracrine factors. The action potential of the MSC-injected region was longer than that of the normoxic PM-injected site and similar to the normal zone of the MSC-engrafted heart. Recently, computer simulation studies showed that myocytes can compensate for the additional electrical load of coupled fibroblasts by increasing the sodium channel current, and a re-flow of this additional charge from fibroblasts to the myocytes occurs during repolarization, consequently increasing APDs (30,31). The MSC-myocyte coupling, which prolongs the myocyte refractory period, may facilitate reentry by creating greater dispersion of repolarization. Nevertheless, this study showed that there was no significant difference in arrhythmogenicity in MSC-engrafted rats compared to normoxic PM-injected rats. In contrast, engraftment of cardiogenic cells reduced arrhythmogenicity by acquiring tissue homogeneity, with no significant change of action potential duration. The PMA, the chemical molecule which we used in order to differentiate the MSCs into cardiogenic cell, involves in alpha-adrenergic signaling and, accordingly, it might cause unexpected other side effect. The further investigation on differentiation into cardiogenic cells or cardiomyocyte with focusing on safely and feasibility in clinical setting should be needed in future.

Study limitations Several study limitations are apparent. First, although we identified several growth factors (IGF, bFGF, and HGF) and Ca^{2+} homeostasis-related proteins, it is possible that other factors are involved. The focus of the present study was the role of environment surrounding stem cells, rather than on the precise mechanism of paracrine factors on arrhythmogeneity. Further studies are needed to identify major factors linking molecular mechanisms of anti-arrhythmic effect from MSCs. Second, the monitoring of survival was limited to a short period of time (11 days), not qualifying as a long term outcome of paracrine factors. This study described ventricular arrhythmia occurring in the early phase of MI, because a therapeutic strategy to target this period is lacking (32), while the risk of sudden arrest or death is highest in the early phase of MI (12).

V. CONCLUSION

Our study showed that in contrast to the negligible proarrhythmic potential of MSCs, paracrine molecules secreted from MSCs had strong antiarrhythmic potential, depending on their surrounding

environment. It is likely that a hypoxic or normoxic environment surrounding MSCs affects the type and properties of the growth factors or cytokines, and these secreted molecules determine the characteristics of the electro-anatomical substrate of the surrounding myocardium. Until now, previous studies have focused mainly on cell types and delivery routes. However, our results demonstrate that paracrine molecules may become a promising option in treating early phase of MI in which antiarrhythmic therapy combined with the protecting effect from tissue damage is required, and cardiomyocyte-like cell, rather than undifferentiated cell, may be another alternative to reduce arrhythmogeneity by overcoming tissue heterogeneity.

REFERENCES

1. Burt RK, Loh Y, Pearce W et al. Clinical applications of blood-derived and marrow-derived stem cells for nonmalignant diseases. JAMA 2008;299:925-36.
2. Chang MG, Tung L, Sekar RB et al. Proarrhythmic potential of mesenchymal stem cell transplantation revealed in an in vitro coculture model. Circulation 2006;113:1832-41.
3. Beeres SL, Zeppenfeld K, Bax JJ et al. Electrophysiological and arrhythmogenic effects of intramyocardial bone marrow cell injection in patients with chronic ischemic heart disease. Heart Rhythm 2007;4:257-65.
4. Gnecchi M, He H, Liang OD et al. Paracrine action accounts for marked protection of ischemic heart by Akt-modified mesenchymal stem cells. Nat Med 2005;11:367-8.
5. Gnecchi M, He H, Noiseux N et al. Evidence supporting paracrine hypothesis for Akt-modified mesenchymal stem cell-mediated cardiac protection and functional improvement. FASEB J 2006;20:661-9.
6. Pak HN, Qayyum M, Kim DT et al. Mesenchymal stem cell injection induces cardiac nerve sprouting and increased tenascin expression in a Swine model of myocardial infarction. J Cardiovasc Electrophysiol 2003;14:841-8.
7. Dangman KH, Dresdner KP, Jr., Zaim S. Automatic and triggered impulse initiation in canine subepicardial ventricular muscle cells from border zones of 24-hour transmural infarcts. New mechanisms for malignant cardiac arrhythmias? Circulation 1988;78:1020-30.
8. Xing D, Martins JB. Triggered activity due to delayed afterdepolarizations in sites of focal origin of ischemic ventricular tachycardia. Am J Physiol Heart Circ Physiol 2004;287:H2078-84.
9. de Bakker JM, van Capelle FJ, Janse MJ et al. Slow conduction in the infarcted human heart. 'Zigzag' course of activation. Circulation 1993;88:915-26.
10. Efimov IR, Huang DT, Rendt JM, Salama G. Optical mapping of repolarization and refractoriness from intact hearts. Circulation 1994;90:1469-80.
11. Kanai A, Salama G. Optical mapping reveals that repolarization spreads anisotropically and is guided by fiber orientation in guinea pig hearts. Circulation research 1995;77:784-802.
12. Solomon SD, Zelenkofske S, McMurray JJ et al. Sudden death in patients with myocardial infarction and left ventricular dysfunction, heart failure, or both. N Engl J Med 2005;352:2581-8.
13. De Ferrari GM, Viola MC, D'Amato E, Antolini R, Forti S. Distinct patterns of calcium transients during early and delayed afterdepolarizations induced by isoproterenol in ventricular myocytes. Circulation 1995;91:2510-5.
14. Fadok VA, Bratton DL, Konowal A, Freed PW, Westcott JY, Henson PM. Macrophages that have ingested apoptotic cells in vitro inhibit proinflammatory cytokine production through autocrine/paracrine mechanisms involving TGF-beta, PGE2, and PAF. J Clin Invest 1998;101:890-8.
15. Beardslee MA, Lerner DL, Tadros PN et al. Dephosphorylation and intracellular redistribution of ventricular connexin43 during electrical uncoupling induced by ischemia. Circulation research 2000;87:656-62.
16. Shaw RM, Rudy Y. Ionic mechanisms of propagation in cardiac tissue. Roles of the sodium and L-type calcium currents during reduced excitability and decreased gap junction coupling. Circulation research 1997;81:727-41.
17. Chang MG, Zhang Y, Chang CY et al. Spiral waves and reentry dynamics in an in vitro model of the healed infarct border zone. Circulation research 2009;105:1062-71.

18. Hahn JY, Cho HJ, Kang HJ et al. Pre-treatment of mesenchymal stem cells with a combination of growth factors enhances gap junction formation, cytoprotective effect on cardiomyocytes, and therapeutic efficacy for myocardial infarction. J Am Coll Cardiol 2008;51:933-43.
19. Doble BW, Kardami E. Basic fibroblast growth factor stimulates connexin-43 expression and intercellular communication of cardiac fibroblasts. Mol Cell Biochem 1995;143:81-7.
20. Peluso JJ. Basic fibroblast growth factor (bFGF) regulation of the plasma membrane calcium ATPase (PMCA) as part of an anti-apoptotic mechanism of action. Biochem Pharmacol 2003;66:1363-9.
21. Aberg ND, Blomstrand F, Aberg MA et al. Insulin-like growth factor-I increases astrocyte intercellular gap junctional communication and connexin43 expression in vitro. J Neurosci Res 2003;74:12-22.
22. Guo Y, He J, Wu J et al. Locally overexpressing hepatocyte growth factor prevents post-ischemic heart failure by inhibition of apoptosis via calcineurin-mediated pathway and angiogenesis. Arch Med Res 2008;39:179-88.
23. Taniyama Y, Morishita R, Aoki M et al. Angiogenesis and antifibrotic action by hepatocyte growth factor in cardiomyopathy. Hypertension 2002;40:47-53.
24. Merriam LA, Scornik FS, Parsons RL. Ca(2+)-induced Ca(2+) release activates spontaneous miniature outward currents (SMOCs) in parasympathetic cardiac neurons. J Neurophysiol 1999;82:540-50.
25. Vannahme C, Smyth N, Miosge N et al. Characterization of SMOC-1, a novel modular calcium-binding protein in basement membranes. J Biol Chem 2002;277:37977-86.
26. Wingo TL, Shah VN, Anderson ME, Lybrand TP, Chazin WJ, Balser JR. An EF-hand in the sodium channel couples intracellular calcium to cardiac excitability. Nat Struct Mol Biol 2004;11:219-25.
27. Yoo SH, Chu SY, Kim KD, Huh YH. Presence of secretogranin II and high-capacity, low-affinity Ca2+ storage role in nucleoplasmic Ca2+ store vesicles. Biochemistry 2007;46:14663-71.
28. Sato D, Xie LH, Sovari AA et al. Synchronization of chaotic early afterdepolarizations in the genesis of cardiac arrhythmias. Proc Natl Acad Sci U S A 2009;106:2983-8.
29. Kardami E, Stoski RM, Doble BW, Yamamoto T, Hertzberg EL, Nagy JI. Biochemical and ultrastructural evidence for the association of basic fibroblast growth factor with cardiac gap junctions. J Biol Chem 1991;266:19551-7.
30. Sachse FB, Moreno AP, Abildskov JA. Electrophysiological modeling of fibroblasts and their interaction with myocytes. Ann Biomed Eng 2008;36:41-56.
31. Xie Y, Garfinkel A, Camelliti P, Kohl P, Weiss JN, Qu Z. Effects of fibroblast-myocyte coupling on cardiac conduction and vulnerability to reentry: A computational study. Heart Rhythm 2009;6:1641-9.
32. Steinbeck G, Andresen D, Seidl K et al. Defibrillator implantation early after myocardial infarction. N Engl J Med 2009;361:1427-36.

APPENDICES

Methods

Isolation and culture of MSCs and neonatal rat ventricular cardiomyocytes. MSCs were purified as previously described (1). Briefly, bone marrow from femoral and tibial bone of 4-week-old male Sprague-Dawley rats (approximately 100 g) was aspirated with 10 ml of Dulbecco's modified Eagle's medium (DMEM) supplemented with 10% fetal bovine serum and 1% antibiotic-penicillin/streptomycin solution. Mononuclear cells recovered after centrifugation in Percoll were washed twice, resuspended in 10% fetal bovine serum (FBS)-DMEM, and plated in flasks at 1 x 10^6 cells per 100 cm^2. Cultures were maintained at 37℃ in a humidified atmosphere containing 5% CO_2. After 48 or 72 hours, non-adherent cells were discarded, and adherent cells were thoroughly washed twice with phosphate-buffered saline (PBS). Fresh complete medium was added and replaced every 3 to 4 days for approximately 10 days. For further purification, the Isolex Magnetic Cell Selection System (Baxter Healthcare Corporation) was used. Briefly, cells were incubated with Dynabeads M-450 coated with anti-CD34 monoclonal antibody. A magnetic field was applied and $CD34^+$ cell-bead complexes were separated from the remaining cell suspension; the CD34-negative fraction was then cultured. Cells were harvested after incubation with 0.25% trypsin and 1 mM EDTA for 5 minutes at 37℃, replated in 1 × 10^5/100-cm^2 plates, and grown for approximately 10 days.

Cardiomyocytes were prepared from Sprague-Dawley neonatal rat hearts. To deplete red blood cells, isolated heart tissues were washed with Dulbecco's phosphate-buffered saline solution (pH 7.4, Invitrogen). Hearts were minced with micro-dissecting scissors to 0.5 mm^3 and treated with 4 ml of collagenase II (1.4 mg/ml; 270 units/mg, Invitrogen) for 5 minutes in a 37℃ humidified chamber. The supernatant was removed and washed with 10% FBS DMEM. Cell pellets were obtained by centrifugation, and resuspended in an equal volume of fresh medium containing 10% FBS. The remaining tissue was treated with fresh collagenase II solution for an additional 5 minutes. The incubation procedure was repeated until the tissue was totally digested. The resulting supernatant was centrifuged at 2000 rpm for 2 minutes at room temperature. The cell pellet was resuspended in 5 ml of cell culture medium and plated for 2 hours at 37℃ in a 5% CO_2 incubator. Non-adherent cells were identified as cardiomyocytes. Unattached cardiomyocytes were replated on 100-mm culture dish (5×10^5cell/ml) and incubated in α-MEM supplemented with 10% FBS. Cells were then cultured in a CO_2 incubator at 37°C. To reduce fibroblast contamination, α-MEM with 0.1mM 5-bromo-2'-deoxyuridine (Brd-U) (Sigma) was used.

Surface ECG. A surface 6-lead ECG was obtained in control, untreated, hypoxic PM- or normoxic PM-treated, MSC-engrafted rats for 5 min. R–R intervals, PR intervals, QRS durations, QT and corrected QT interval were measured by successe evaluation. All data were acquired at a 1 ksps (kilo-sample per second) using the Bard stamp amplifier System (C.R. Bard Inc.).

ECG Telemetry. To monitor ambulatory electrocardiographs, radio frequency transmitters (TR50B, Telemetry research, USA) were implanted and recorded data was analyzed with LabChart™ software.

Systemic administration of isoproterenol. Isoproterenol (2 mg/kg) was injected intraperitoneally after surface 6 lead electrocardiography leads (limbs). The number of episodes of premature ventricular contractions during the 20 minutes immediately after injection was calculated.

Left ventricular catheterization. For invasive hemodynamics, left ventricular catheterization was performed at 7 to 11 d after operation. Millar Mikro-tip 2 F pressure transducer (model SPR-838, Millar Instruments, Houston, TX) was introduced into the left ventricle via the right carotid artery under zoletil (20 mg/kg) and xylazine (5 mg/kg) anesthesia. Real-time pressure-volume loops were recorded by a blind investigator and all data were analyzed off-line with PVAN 3.5 software (Millar).

VT induction experiment protocol. Electrical stimuli of two times diastolic threshold were delivered through bipolar electrodes at the non-infarcted zone of the LV base. The ventricles initially were paced at a constant pacing cycle length (CL) of 260 ms. After 15 to 20 stimuli had been delivered at this pacing CL, optical images were acquired. The pacing cycle length was shortened by 20 ms decrements for a pacing CL of 200 ms and by 10 ms decrements for a pacing CL <200 ms until a pacing CL of 90 ms or induction of VT. ECGs were continuously monitored using the Biopac System (BIOPAC Systems Inc., Aero Camino Goleta, CA). VT susceptibility score was defined as following; score 0= no induction, score 1= VT at a pacing CL of < 110ms, score 2 = VT at a pacing CL of <160ms, score 3= VT at a pacing CL of <200ms, score 4 = VT at a pacing CL of more than 200ms or spontaneous VT induction.

Histological analysis for myocardial fibrosis area and apoptotic cell death. The heart was fixed in 10% formalin solution (Sigma Aldrich, St. Louis, MO) for 24 hours at 4℃. Paraffin blocks were made and 2-μm slides were prepared with Masson's trichrome staining. Interstitial fibrosis was measured with MetaMorph software version 4.6 (Universal Imaging Corporation Ltd., United Kingdom). The TUNEL assay was performed according to the manufacturer's instructions (Chemicon International Inc., Temecula, CA). In brief, five micrometer-thick tissue sections were deparaffinized, rehydrated, and rinsed with PBS. Sections were pretreated with 3.0% H_2O_2, subjected to TdT enzyme reaction at 37℃ for 1 hour and incubated with digoxigenin-conjugated nucleotide substrate at 37℃ for 30 minutes. Nuclei exhibiting DNA fragmentation were stained with 3,3-diamino benzidine (DAB) (Vector Laboratories, INC., Burlingame, CA) for 5 minutes. Sections were observed by light microscopy; six slices per group were prepared, with 10 regions observed on each slice (× 400).

Immunohistochemistry. The heart was perfusion-fixed with 10% (v/v) neutral buffered formaldehyde for 24 hrs, transversely sectioned into 4 comparably thick sections and embedded in paraffin by routine methods. Sections of 2 um-in thickness were mounted on a gelatin-coated glass slides to ensure different stains could be used on successive sections of tissue cut through the

implantation area. After de-paraffinization and re-hydration, the sections were stained with rabbit polyclonal anti-connexin 43 and mouse monoclonal anti-connexin 43 from Zymed Laboratories Inc. (South San Francisco, CA) and then with secondary antibodies. A rabbit polyclonal anti-Cx43 (Zymed Laboratories Inc, South San Francisco, CA), was used to identify the total amount of Cx43. A mouse monoclonal antibody (Zymed Laboratories Inc, South San Francisco, CA) was used to identify dephosphorylated Cx43. All images were made by using an excitation filter under reflected light fluorescence microscopy and transferred to a computer equipped with MetaMorph software version 4.6 (Universal Imaging Corp.).

Immunocytochemistry. Anti-Cx43 antibodies were used to detect changes in total and dephosphorylated Cx43 in ischemic cardiomyocytes with treatment of control DMEM (CTL-M), hypoxic PM, or normoxic PM. After ischemia 3hr and oxygenation following treatment, of which *in vitro* model may mimic *in vivo* model, monolayers were removed from the bath apparatus and fixed with 2% formaldehyde for 10 minutes in 0.1 mmol/L Ca^{2+} Tyrode's solution. Monolayers were incubated with protein block solution and then exposed to either monoclonal (against dephosphorylated Cx43) or polyclonal (against total Cx43) primary antibodies for 1 hour and with secondary antibodies for 45 minutes. Finally, monolayers were treated with DAPI (Sigma, St Louis, Mo) to stain nuclei for 2 minutes and then mounted on slides. All slides were viewed on an epifluorescence microscope and digitally photographed for later analysis.

Immunocytochemical characterization of MSCs is demonstrated below. Cells were cultured in a 4-well slide chamber, washed with PBS, and incubated in 1% paraformaldehyde solution for 10 min. The cells were then washed twice with PBS before being permeabilized in 0.1% Triton X-100 for 7 min. After this, the cells were blocked for 1 h (blocking solution: 2% bovine serum albumin and 10% horse serum in PBS) and then stained with the appropriate antibodies. FITC-conjugated mouse, rabbit, and goat (Jackson Immunoresearch Laboratories) secondary antibodies were used. Immunofluorescence was detected with confocal microscopy (Carl Zeiss).

Measurement of Cytosolic Free Ca^{2+}. The measurement of the cytosolic free Ca^{2+} concentration was performed by confocal microscopy analysis. Neonatal rat cardiomyocytes were plated on a four-well slide chamber coated with 1.5% gelatin for 1 day in α-MEM containing 10% fetal bovine serum (Gibco BRL) and 0.1 μM BrdU (Sigma). After incubation, cells were washed with modified Tyrode's solution with 0.265 g/L $CaCl_2$, 0.214 g/L $MgCl_2$, 0.2 g/L KCl, 8.0 g/L NaCl, 1 g/L glucose, 0.05 g/L NaH_2PO_4, and 1.0 g/L $NaHCO_3$. Cells were then loaded with 10 μM acetoxymethyl ester fluo-4 (Fluo-4 AM, Molecular Probe) for 20 minutes, at 37℃, in the dark. Fluorescence images were collected using confocal microscope excited by a 488-nm argon laser and emitted light was collected through a 510-560 nm band-pass filter. The relative intracellular Ca^{2+} concentration was determined by measuring fluorescent intensity.

Proteomic analysis. Conditioned media with paracrine factors was constituted in acid cleavable isotope-coded affinity tag (ICAT)-labeling buffer, including light or heavy isotopes (5). The mixture was incubated in the dark area for 100 min at room temperature. The sample was digested with trypsin at 37℃ overnight, was separated by cation-exchange chromatography, and then purified by avidin-affinity chromatography. Final samples were analyzed by microcapillary HPLC-electrospray ionization-mass spectrometry (ESI-MS/MS) (5). Peptide fragmentation data was searched by using SEQUEST. Quantification and data analysis were resulted from ProteinProphet software (6). All peptide were normalized to adjust for any systematic error.

RT-PCR. The expression levels of various genes were analyzed by reverse transcription polymerase chain reaction (RT-PCR). Total RNA was extracted with 500 μl Tri-reagent per 60 mm plate (Sigma). We poured 100 μl of chloroform over the Tri-reagent and vortexed each sample for about 10 secs. The sample was then centrifuged at 12,000 g and 4℃ for 15 min. After this, three layers appeared in the tube, and the upper transparent layer was collected to new tubes. Thereafter, 250 μl of 2-propanol was added to the sample, and the mixture was again vortexed for about 30 sec, followed by centrifugation at 12,000 g and 4℃ for 10 min. Next, the supernatant was discarded, and the pellet was washed with 75% ethanol (Duksan) mixed with diethylpyrocarbonate (DEPC; Sigma) water. At this point, centrifugation was done at 7,500 g and 4℃ for 5 min, and the pellet was dried at room temperature for about 7 min. Finally, 30 μl of nuclease free water was added. The quality and quantity of the RNA were detected with the OD_{260}/OD_{280} value using a DU 640 spectrophotometer (Eppendorf). Complementary DNA was generated with the Reverse Transcription System (Promega) according to the manufacturer's instructions. One μg of total RNA was reverse-transcribed in a 20 μl reaction mix containing 5 mmol/L $MgCl_2$, 10 mmol/L Tris-HCl (pH 9.0 at 25℃), 50 mmol/L KCl, 0.1% Triton X-100, 1 mmol/L dNTPs, 20 U of RNase inhibitor, 0.5 μg oligo-$(dT)_{15}$ primer, and 10 U of reverse transcriptase for 15 min at 42℃, and the reaction was terminated by heating at 99℃ for 5 min. The PCR mix contained 10 pmol/μl of each primer, together with 200 mM Tri-HCl (pH 8.8), 100 mM KCl, 1.5 mmol/L $MgSO_4$, 1% Triton X-100, 0.1 mM dNTPs, and 1.25 U of Taq polymerase in a total volume of 25 μl. PCR conditions consisted of a cycle of denaturing at 94℃ for 3 min, and followed by 35 cycles of denaturation at 94℃ for 30 sec, annealing at 49℃ for 30 sec, and extension at 72℃ for 2 min before a final extension at 72℃ for 10 min. RT-PCR products were separated by electrophoresis in a 1.2% agarose gel, and visualized after staining with ethidium bromide.

Appendix Figure 1. Numbers of premature ventricular contractions (PVCs) recorded with a telemetric/ECG monitoring (*p<0.01).

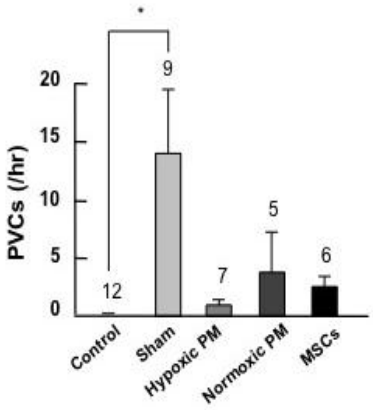

Appendix Figure 2. VT vulnerability score by ANCOVA test adjusted for LV ejection fraction (*p<0.001).

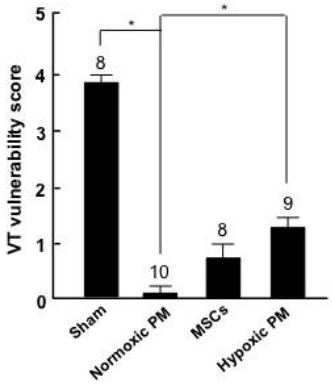

Appendix Figure 3. Sequential di-4-ANNEPS fluorescence images of action-potential propagation in sham- (upper, n=9), hypoxic PM- (upper middle, n=6), normoxic PM- (lower middle, n=6), and MSCs- (lower, n=8) injected hearts. The infarct region is outlined by a white circle. The activation bypasses the infarct, whereas it proceeds through the PM-injected lesion. Conduction delays occur in the normoxic PM- or MSCs-injected lesion.

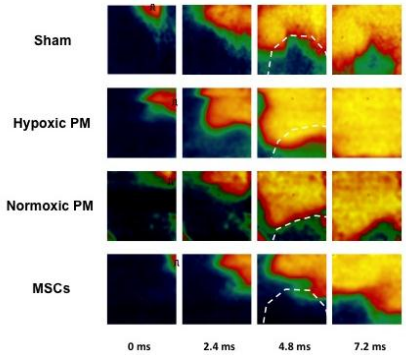

Appendix Figure 4. Representative photographs of cardiomyocytes grown under normoxic (A) or treatment of control (B), hypoxic PM (C), or normoxic PM (D) following hypoxia 3hrs (*p <0.01,**p <0.001).

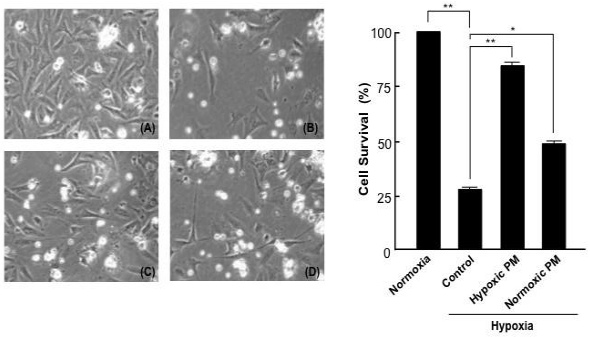

Appendix Figure 5. Alteration of Ca^{2+}-regulatory ion channels and proteins *in vitro* study. Effect of PM on genes coding for ion exchangers and Ca^{2+}-regulating proteins. The mRNA levels of NCX, SERCA2A, LTCC, Na^+/K^+ ATPase, calreticulin, and calmodulin were examined by RT-PCR (*p <0.01, **p <0.001).

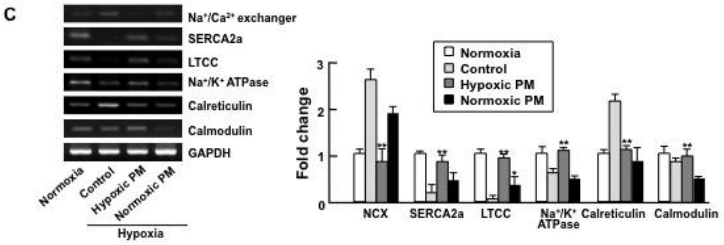

Appendix Figure 6. The concentration of bFGF and IGF-1 quantified by ELISA assay. (**p<0.001).

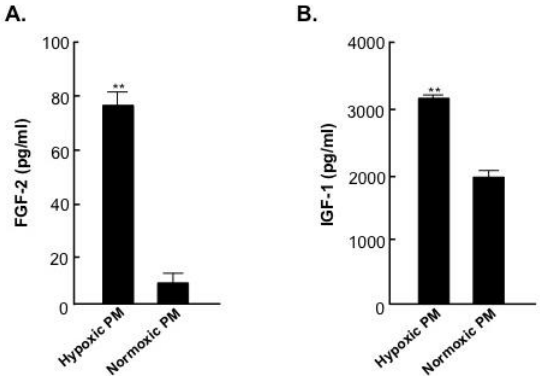

Appendix Figure 7. The altered expression levels of cardiac specific markers, cTnT, MLC, MHC, MEF2, and NkX2.5 in the cardiogenic cells. Values were normalized against values from MSCs control and are the mean ± SEM of three independent experiments.

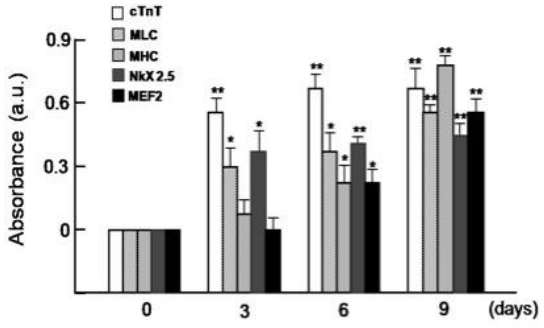

Appendix Table 1. Paracrine factors differentially secreted between hypoxic PM and normoxic PM

Protein name (entry)	ID[a)]	Proposed Function	Ratio (H/N)[b)]	SD	Unique peptide identified
Fibroblast growth factor 2 (Q7TPG9)	**Q7TPG9_MOUSE**	**Gap junction, cell proliferation**	**6.5**	**0.42**	**1**
Insulin-like growth factor 1 (P05017)	**IGF1_MOUSE**	**Gap junction, cytoprotection**	**2.1**	**0.45**	**1**
Hepatocyte growth factor (Q08048)	**HGF_MOUSE**	**Cell proliferation**	**1.8**	**0.48**	**1**
EF hand domain containing 2* (Q9CQ46)	**EFCB2_MOUSE**	**Calcium regulation**	**-**	**-**	**5**
Reticulocalbin 2* (Q8BP92)	**RCN2_MOUSE**	**Calcium regulation**	**-**	**-**	**3**
Secreted modular calcium-binding protein 1* (Q8BLY1)	**SMOC1_MOUSE**	**Calcium regulation**	**-**	**-**	**1**
Secretogranin II* (Q03517)	**SCG2_MOUSE**	**Calcium regulation**	**-**	**-**	**1**

[a)] Protein Knowledgebase (UniProtKB): www.uniprot.org

[b)] Hypoxic PM/Normoxic PM

* Detected in hypoxic PM, but not in normoxic PM

ABSTRACT (IN KOREAN)

심근경색 모델에서 중간엽 세포, 분비액, 분화된 세포가 미치는 항부정맥, 부정맥 효과

<지도교수 이문형>

연세대학교 대학원 의학과

황혜진

줄기세포의 심장 이식이 부정맥을 일으키는지에 대한 논란이 많이 있었다. 본 연구는 중간엽 줄기세포와 줄기세포의 분비액, 그리고 심세포로 분화된 세포가 심장에 이식되었을때, 어떠한 항부정맥 또는 부정맥 효가를 나타내는지 조사함. 쥐심근경색 모델을 이용하여 중간엽줄기세포, 심근세포 분화된 세포 및 분비액(저산소 및 정상대기에서 각각 나온 분비액)을 주입한 네 군에서 생존분석, 전기생리 검사, 광학적 매핑, 조직학, 면역조직형관 분석을 이용하여 비교하였다. 중간엽 줄기세포 주입한 군과 정상산소 환경에서 나온 배양액만 처리한 군을 비교할 때 생존율에서 차이가 없었고, 심근경색 모델에 비해 생존율은 약간 증가하는 경향을 보. 또한 전기생리검사에서 부정맥 발생 정도가 비슷하였으며, 광학 매핑상에서 전기전도 속도가 경색부위에서 약간 호전되는 양상을 보였고 Connexin 43발현이 약간 증가 하는 양상 보. 이에 비해 저산소 환경에서 나온 만 처리한 군과 심근세포계열로 분화시킨 세포를 주입한 전기전도 속도도 매우 증가함. 특히 저산소환경에서 나온 분비액만 주입한 군에서는 Cx43 발현 증가, Calcium signaling관련 단백질 발현이 증가하여, 결과적으로 전기생리검사상 부정맥 양상이 줄어드는 것으로 나타남. 이는 fibroblast growth factor, insulinlike growth factor 1, hepatocyte growth factor, and EFhand domain-containing 2가 gap junction 및 칼슘 관련 단백질 발현에 영향을 주는 것으로 나타남. 결론적으로 저산소 상태에서 나온 중간엽 줄기세포의 분비액과 심근세포로 분화한 세포의 이식은 조직의 이질성을 줄이고 동질성을 획득하여 항부정맥 효과를 나타냄.

핵심되는 말 : 심근경색, 심실부정맥, 중간엽 줄기세포, 줄기세포 분비액

PUBLICATION LIST

1. Song H, Hwang HJ, Chang W, Song BW, Cha MJ, Kim IK, Lim S, Choi EJ, Ham O, Lee CY,Park JH,Lee SY,Choi E,Lee C,LeeM,Lee MH,Kim SH,Jang Y,Hwang KC. Cardiomyocytes from phorbolmyristateacetate-activated mesenchymal stem cell restore electromechanical function in infarcted rat hearts. Proc Natl Acad Sci U S A. 2011 Jan 4;108(1):296-301

2. Hwang HJ, Chang W, Song B, Song H, Cha M, Kim I, Lim S, Choi E, Ham O, Lee S, Shim J, et al. Antiarrhythmic Potential of Mesenchymal Stem Cell Is Modulated by Hypoxic Environment. J Am Coll Cardiol. 2012 Oct 23;60(17):1698-706.